Carcinogenesis vol.31 no.2 pp.239–245, 2010
doi:10.1093/carcin/bgp174
Advance Access publication July 22, 2009

Inhibition of vinyl carbamate-induced pulmonary adenocarcinoma by indole-3-carbinol and *myo*-inositol in A/J mice

Fekadu Kassie[1,2,*], Stephen Kalscheuer[1], Ilze Matise[1], Linan Ma[3], Tamene Melkamu[2], Pramod Upadhyaya[1] and Stephen S.Hecht[1]

[1]Masonic Cancer Center, Mayo Mail Code 806, 420 Delaware Street Southeast, Minneapolis, MN 55455, USA, [2]College of Veterinary Medicine, University of Minnesota, MN 55108 and [3]Biostatistics and Informatics Core, University of Minnesota, MN 55455, USA

*To whom correspondence should be addressed. Tel: +1 612 625 9637; Fax: +1 612 626 5135;
Email: kassi012@umn.edu

In previous studies, we reported that indole-3-carbinol (I3C) and *myo*-inositol (MI) inhibit lung adenoma induced by tobacco smoke carcinogens in A/J mice. In this paper, we extended our work and examined the effects of I3C (70 or 30 μmol/g diet) and MI (56 μmol/g diet) against vinyl carbamate (VC)-induced lung adenocarcinoma by administering the agents from 1 week after the second of two injections of VC until termination of the study at week 18. The higher dose of I3C decreased multiplicities of tumors on the surface of the lung (26%, $P = 0.0005$), carcinoma incidence (38%), multiplicity (67%, $P < 0.0001$) and size (complete abolition of carcinoma with an area of >1.0 cm^2) as well as adenoma with cellular pleomorphism (46%, $P < 0.0001$). The lower dose of I3C was less effective. MI decreased multiplicities of pulmonary surface tumors (20%, $P = 0.0005$), adenoma with cellular pleomorphism (40%, $P < 0.0001$) and lung adenoma (52%, $P < 0.0001$) and the proportion of the biggest carcinoma (carcinoma with an area of >1.0 cm^2, $P < 0.05$). Immunoblot analyses of lung tissues for potential target identification showed that I3C (70 μmol/g diet) inhibits IkappaBα degradation, nuclear factor-kappaB activation, expression of cyclooxygenase-2, phospho-Akt and fatty acid synthase (FAS) and activates caspase-3 and poly ADP ribose polymerase cleavage. The effect of MI was limited to inhibition of phospho-Akt and FAS expression. Our data show that I3C and MI inhibit lung carcinoma and provide a basis for future evaluation of these compounds in clinical trials as chemopreventive agents for current and former smokers.

Introduction

Lung cancer is the most common cancer-related death worldwide (1). In the USA, an estimated 215 020 new cases and 161 840 deaths were expected in 2008, accounting for 15% of cancer diagnoses and 29% of all cancer deaths, respectively (2). The 5 year survival rate of lung cancer is estimated to be 15% in USA and 10% in Europe (1), clearly indicating the need for prevention of lung cancer. One promising approach is development of effective chemopreventive agents for both current and former smokers.

Plant foods are rich in cancer preventing phytochemicals. Among the phytochemicals commonly consumed in plant foods are indole-3-carbinol (I3C), a compound found in *Brassica* vegetables as glucobrassicin, and *myo*-inositol (MI), a constituent of a wide variety of foods such as whole grains, seeds and fruit. Considerable evidence shows that I3C inhibits experimentally induced and spontaneous tumors in multiple tissues, including lung, through induction of phase I and II enzymes, inhibition of proliferation of tumor cells, induction of apoptosis in tumor cells and modulation of estrogen metabolism (3).

Abbreviations: Cox-2, cyclooxygenase-2; DIM, 3,3′-diindolylmethane; FAS, fatty acid synthase; I3C, indole-3-carbinol; MI, *myo*-inositol; NF-κB, nuclear factor-kappaB; PARP, poly ADP ribose polymerase; VC, vinyl carbamate.

Moreover, I3C inhibited breast cancer bone metastasis in severe combined immunodeficient mice (4). Most of the biological activities of I3C are attributed to 3,3′-diindolylmethane [(DIM) (5)], an acid-catalyzed condensation product of the parent compound formed in the acidic milieu of the stomach. DIM caused anticarcinogenic effects in animal models and inhibited cell proliferation and induced apoptosis in several cancer cell lines by modulating the expression of several signaling proteins (6–10). Moreover, DIM inhibited migration in cell culture and decreased blood vessel formation in xenograft models (11,12). When given before chemotherapeutic drugs, DIM chemosensitized pancreatic cancer cells to these agents via suppression of drug-induced activation of nuclear factor-kappaB (NF-κB) (13).

MI is one of the most promising dietary agents for the prevention of lung cancer. Besides its efficacy, it has negligible toxicity. MI inhibited lung tumorigenesis in A/J mice exposed to the tobacco smoke carcinogens benzo[*a*]pyrene, 4-(methylnitrosamino)-1-(3-pyridyl)-1-butanone or a combination of the two (14–17). MI also increased the rate of regression of pre-existing dysplastic lesions in former smokers (18). The mechanisms for the cancer preventive effects of MI are not well known, but this compound was shown to reverse cell differentiation inhibitory effects of anti-7,8-dihydroxy-9,10-epoxy-7,8,9,10-tetrahydrobenzo[*a*]pyrene (19) and inhibit Akt and extracellular signal-regulated kinase expression (20).

In previous studies, we reported the efficacy of I3C and MI to inhibit 4-(methylnitrosamino)-1-(3-pyridyl)-1-butanone plus benzo [*a*]pyrene-induced lung adenoma in mice (21–23). In the present study, we extended the earlier work to investigate inhibition of vinyl carbamate (VC)-induced lung adenocarcinoma by the chemopreventive agents. Moreover, we examined potential mechanisms for the lung cancer inhibitory activities of I3C and MI.

Materials and methods

Chemicals, reagents and diets

I3C, MI and a cocktail of protease inhibitors were from Sigma (St Louis, MO). VC was purchased from Toronto Research Chemicals (Ontario, Canada). Anti-cyclooxygenase-2 (Cox-2), anti-phospho-Akt (343), anti-caspase-3, anti-poly ADP ribose polymerase (PARP), anti-β-actin and goat anti-rabbit IgG were from Santa Cruz Biotechnology (Santa Cruz, CA). Anti-fatty acid synthase (FAS), anti-phospho NF-κB and anti-IkappaBα were from Cell Signaling Technology (Beverly, MA). Mouse diets (AIN-93G and AIN-93M) were purchased from Harlan Teklad (Madison, WI). The AIN-93G diet, high in protein and fat, was used to support rapid growth of the mice during early age, whereas AIN-93M diet, low in protein and fat, was used for maintenance.

Animal studies

Female A/J mice, 5–6 weeks of age, were obtained from The Jackson Laboratory (Bar Harbor, ME). The experimental design is shown in Figure 1. Upon arrival, the mice were housed in the specific pathogen-free animal quarters of Research Animal Resources, at University of Minnesota Academic Health Center and maintained on AIN-93G pellet diet. One week after arrival, the mice were randomized into different groups and shifted to AIN-93G powder diet. The mice in groups 1–4 received two intraperitoneal injections of VC (0.32 mg per mouse in 0.1 ml isotonic saline) one week apart. One week after the second carcinogen dose, mice in groups 2, 3 and 4 were given AIN-93M diet supplemented with 70 μmol I3C/g diet, 30 μmol I3C/g diet or 56 μmol MI/g diet, respectively, whereas mice in group 1 (carcinogen control) were maintained on non-supplemented AIN-93M diet. The doses of the chemopreventive agents were determined on the basis of results from our previous studies (16,22). The mice in group 5 were injected with the vehicle only (physiological saline) and received non-supplemented AIN-93M diet (Figure 1). The experiment was terminated at week 18 and lungs were removed. Surface tumors were counted under a dissecting microscope. The whole left lobe of the lung (vehicle-treated group) or the tumors microdissected thereof (carcinogen-treated mice) were kept at −80°C for western immunoblotting analysis. The

remaining four lung lobes were preserved in 10% buffered formalin for histopathological studies.

Histopathological analysis

Randomly selected, formalin-fixed lung tissues were processed through a series of graded alcohols, embedded in paraffin and three step sections (each 200 μm apart) having a thickness of 4 μm were cut and stained with hematoxylin and eosin. Proliferative lesions were counted in each step section and the total number of each type of lesion per mouse was expressed as an average number of each lesion per section (sum of each lesion in three step sections divided by three).

Proliferative lesions in the lungs were classified as hyperplasia, adenoma or adenocarcinoma based on recommendations published by the Mouse Models of Human Cancers Consortium (24). The category 'adenoma with cellular pleomorphism' (also known as adenoma with dysplasia and adenoma with progression) was added based on our experience and previously published literature: an adenoma in which ≥10 cells are pleomorphic, characterized by large cell and/or nuclear size; increased cytoplasmic-to-nuclear ratio; prominent nucleoli; nuclear crowding and increased numbers of mitotic figures with no evidence of parenchymal invasion by pleomorphic cells (25,26).

To determine the size of pulmonary adenocarcinoma, first, digital images of the lesions were taken with a Spot Insight 4 digital camera attached to a Nikon Eclipse light microscope and saved as tiff files. The highest magnification that included the entire tumor in one field was used (usually with ×10 objective but ×20 or ×4 objectives were used for smaller and larger tumors, respectively). Subsequently, the tumor size was determined with the Image Pro program precalibrated to convert pixels into square microns according to magnification used for acquiring the image. In Image Pro, the tumor was outlined with a free hand drawing tool, the area was converted into a single object and the size of this object measured in square microns. These data were imported into an Excel file.

Western immunoblot analyses

Aliquots of normal lung tissues (30 mg per mouse) or microdissected tumors (30 mg per mouse) from six mice were pooled and homogenized in ice-cold lysis buffer [50 mmol/l Tris–HCl, 150 mmol/l NaCl, 1 mmol/l ethyleneglycol-bis(aminoethylether)-tetraacetic acid, 1 mmol/l ethylenediaminetetraacetic acid, 20 mmol/l and 1% Triton X-100 (pH 7.4)] containing protease inhibitors [aprotinin (1 μg/ml), leupeptin (1 μg/ml), pepstatin (1 μmol/l) and phenylmethylsulfonyl fluoride (0.1 mmol/l)] and the phosphatase inhibitors Na_3VO_4 (1 mmol/l) and NaF (1 mmol/l). After the homogenates had been centrifuged (14 000*g* for 25 min at 4°C), the supernatants were collected, aliquoted and stored at −80°C. For western immunoblotting, 60 μg of protein per sample were loaded onto a 4–12% Novex Tris–glycine gel (Invitrogen, Carlsbad, CA) and run for 60 min at 200 V. The proteins were then transferred onto a nitrocellulose membrane (Bio-Rad, Hercules, CA) for 1 h at 30 V. Protein transfer was confirmed by staining membranes with BLOT-FastStain (Chemicon, Bill-Erica, MA). Subsequently, membranes were blocked in 5% Blotto non-fat dry milk in Tris buffer containing 1% Tween 20 for 1 h and probed overnight with the following primary antibodies: anti-COX-2 (1:200), anti-phospho-Akt (1:100), anti-FAS (1:1000), anti-phospho NF-κB (1:1000), anti-IkappaB, (1:1000), anti-PARP (1:1000) and anti-β-actin (1:200). After incubating the membranes with a secondary antibody (goat anti-rabbit IgG; 1:10 000) for 1 h, chemiluminescent immunodetection was used. Signal was visualized by exposing membranes to HyBolt CL autoradiography film. All membranes were stripped and reprobed with anti-β-actin to check for differences in the amount of protein loaded in each lane. For each protein, at least three western assays were carried out.

Statistical analysis

The results of gross tumor counts and microscopic lesions per mouse were summarized as mean and standard deviation. The effects of the chemopreventive agents on surface tumors are shown as a percent change in tumor multiplicity in carcinogen plus I3C or MI groups relative to the group treated with carcinogen only. Statistical comparisons among the groups were done using Poisson regression, which is specific for data representing counts or number of events and can handle cases where few or no events occur. Microscopic lesions were analyzed by regression analyses after the data were adjusted for the number of sections and mice associated with each specimen. $P < 0.05$ was used to determine statistical significance.

Results

Effect of I3C and MI on body weight gain

Observation of the mice once a week for signs of toxicity, such as changes in fur color or texture, motor and behavioral abnormalities and palpable masses, did not reveal any of these effects. Mice in the different treatment groups had similar body weights before the beginning of dietary treatment (∼16.5 g). However, the final body weights of mice given I3C at dose levels of 30 μmol/g diet and 70 μmol/g diet were reduced by 6 and 10%, respectively, compared with the body weight of mice treated with the carcinogen alone (Table I). This effect was not due to reduced food intake since the average food consumption of mice maintained on I3C-supplemented diet was ∼9% higher

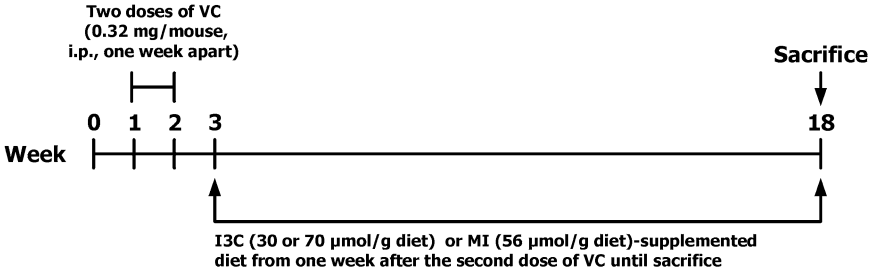

Fig. 1. Experimental design to assess inhibition of VC-induced lung adenocarcinoma in A/J mice by I3C and MI.

Table I. Effects of I3C and MI on VC-induced lung tumor incidence and multiplicity in A/J mice[a]

Group	Carcinogen	Chemopreventive agent (dose, μmol/g diet)	No. of mice	Mean body weight		Lung tumors			
				Initial	At termination	Tumor incidence (%)	Tumors per mouse (mean ± SD)	Reduction in tumor multiplicity (%)	P[b]
1	VC	—	21	16.5 ± 0.6	22.1 ± 1.3	100	42.6 ± 11.9	—	—
2	VC	I3C (70)	20	16.3 ± 0.9	19.9 ± 1.8	100	31.6 ± 4.8	26	0.0003
3	VC	I3C (30)	20	16.6 ± 0.4	20.8 ± 1.6	100	43.5 ± 8.1	None	
4	VC	MI (56)	20	16.4 ± 0.8	22.7 ± 1.1	100	33.9 ± 6.1	20	0.0005
5	None	None	10	16.3 ± 0.5	23.3 ± 1.8	10	0.1 ± 0.3	—	—

[a]Beginning at age 6–7 weeks, groups of female A/J mice were injected intraperitoneally with two doses of VC 1 week apart. The mice were maintained on AIN-93G diet from age 5–6 weeks until 1 week after the end of carcinogen treatment and then shifted to AIN-93M diet for the duration of the experiment. I3C or MI was added to the diet beginning 1 week after the second dose of the carcinogen. The experiment was terminated 15 weeks after the second dose of the carcinogen.
[b]Compared with Group 1.

than that of the group maintained on non-supplemented diet (data not shown). The body weights and food consumption of mice given MI-supplemented diet were similar to those of the group treated with VC and maintained on non-supplemented diet.

I3C and MI reduced the multiplicity of VC-induced pulmonary surface tumors

As shown in Table I, mice treated with VC and fed non-supplemented diet had 42.6 ± 11.9 lung tumors per mouse. Carcinogen-treated mice given I3C at a level of 70 μmol/g diet had 31.6 ± 4.8 tumors per mouse, corresponding to a reduction by 26% ($P = 0.0003$), whereas the lung tumor multiplicity of mice maintained on diet containing the lower dose of I3C (30 μmol/g diet) was similar to that of mice treated with the carcinogen alone (43.5 ± 8.1 tumors per mouse). Dietary administration of MI (56 μmol/g diet) significantly reduced VC-induced lung tumor multiplicity to 33.9 ± 6.1, corresponding to a reduction by 20% ($P = 0.0005$). The multiplicity of spontaneous tumors in vehicle-treated mice was 0.1 ± 0.3 tumors per mouse, which is similar to what was reported earlier by us and others. Surface lung tumor incidence was reduced by neither of the chemopreventive agents. This was not unexpected since the most sensitive indicator in the A/J mouse lung tumorigenesis model is tumor multiplicity.

Upon counting the lung tumors, the diameter of the tumors was categorized into three classes: >2 mm, 1–2 mm and <1 mm. Most of the tumors, regardless of treatment, had a diameter of <1 mm. In the group treated with the carcinogen only, multiplicities of lung tumors having a diameter of >2 mm, 1–2 mm and <1 mm were 0.7 ± 0.9, 16.4 ± 8.3 and 25.4 ± 6.8 tumors permouse, respectively. The higher dose of I3C (70 μmol/g diet) decreased multiplicities of lung tumors with a diameter of >2 mm and 1–2 mm to 0.05 ± 0.08 tumors per mouse ($P = 0.017$) and 2.8 ± 2.0 tumors per mouse ($P < 0.001$), respectively, but not the smallest tumors (28.8 ± 9 tumors per mouse, Figure 2). The lower dose of I3C (30 μmol/g diet) did not affect the multiplicity of any of the size categories of lung tumors. In mice given MI, only the multiplicity of lung tumors with a diameter of 1–2 mm was significantly reduced (6.7 ± 2.3 tumors per mouse, $P < 0.001$).

Effect of I3C and MI on incidence and multiplicity of microscopic pulmonary lesions

Microscopic lesions observed in lung tissues of mice were classified as hyperplastic foci, adenoma, adenoma with cellular pleomorphism and adenocarcinoma based on established criteria (24). Images of representative lung tissue sections showing the various microscopic lesions are depicted in Figure 3. The incidence of pulmonary hyperplastic foci, adenoma and adenoma with cellular pleomorphism was 100% in all carcinogen-treated groups irrespective of dietary supplementation. The incidence of pulmonary adenocarcinoma was 100% in mice treated with the carcinogen alone or carcinogen plus MI but was reduced to 80 and 62% in mice given the lower and higher doses of I3C, respectively (data not shown).

As shown in Table II, multiplicities of hyperplastic foci, adenoma, adenoma with cellular pleomorphism and adenocarcinoma in mice treated with carcinogen only were 1.7 ± 1.6, 4.6 ± 2.1, 3.5 ± 1.6 and 0.6 ± 0.8, respectively. The higher dose of I3C reduced the multiplicities of adenoma with cellular pleomorphism (1.9 ± 1.5, $P < 0.0001$) and adenocarcinoma (0.2 ± 0.5, $P = 0.04$) but not multiplicities of hyperplastic foci or adenoma. The lower dose of I3C reduced only the multiplicities of adenoma with cellular pleomorphism (2.5 ± 1.8, $P < 0.0001$). In mice given MI lower multiplicities of adenoma (2.2 ± 1.6, $P < 0.0001$) and adenoma with cellular pleomorphism (2.1 ± 1.2, $P < 0.0001$) were observed.

Effect of I3C and MI on the size of pulmonary adenocarcinoma

Upon determining the diameter of tumors on the surface of the lung, we noticed that the frequency of larger tumors was reduced by I3C and MI. On the basis of this observation, we asked if the chemopreventive agents decreased the size of pulmonary adenocarcinoma as well. To answer this question, the total area of each adenocarcinoma lesion was measured using the Image Pro program and the size of the tumors grouped into three classes: <0.1 cm^2, 0.1–1. 0 cm^2 and >1.0 cm^2. The results of this study are presented in Table III. In the group treated with carcinogen only, no carcinoma had an area <0.1 cm^2, whereas 22 carcinoma (63%) measured 0.1–1. 0 cm^2 and the remaining 13 carcinoma (37%) had an area of >1.0 cm^2. In mice treated with the carcinogen and given the higher dose of I3C, 36% of the carcinoma measured <0.1 cm^2 and the proportion of carcinoma with an area of 0.1–1. 0 cm^2 was similar to the group given carcinogen only (64%), but no carcinoma with an area >1.0 cm^2 was observed. In mice treated with VC and given the lower dose of I3C or MI, compared with the group treated with the carcinogen only, the proportion of tumors with an area of 0.1–1. 0 cm^2 was significantly increased ($P < 0.05$), whereas that of the biggest tumors (>1.0 cm^2) was significantly reduced ($P < 0.05$).

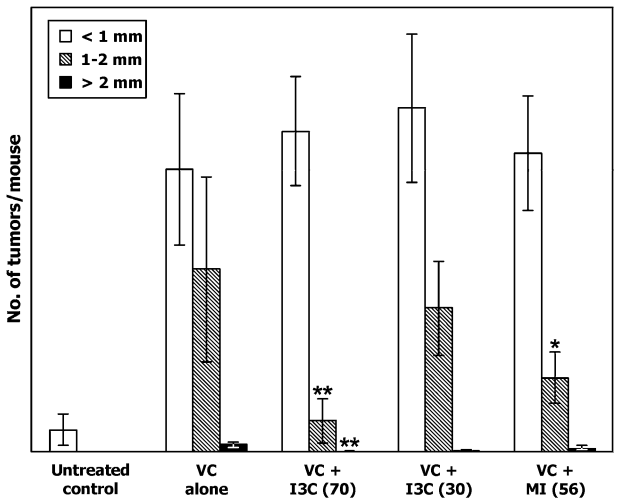

Fig. 2. Effect of I3C and MI on growth of lung tumors. The size of surface tumors on lungs of mice was estimated using the calibrated scale in the eyepiece of a dissecting microscope. Each tumor was assigned to one of the following categories: <1 mm, 1–2 mm and >2 mm. The results show the multiplicity of tumors of the different size categories in mice treated with vehicle, VC alone, VC plus I3C (70 μmol/g diet), VC plus I3C (30 μmol/g diet) and VC plus MI (56 μmol/g diet); $^{*}P = 0.017$ and $^{**}P < 0.001$.

Inhibition of VC-induced IkappaBα degradation, NF-κB activation and Cox-2 expression by I3C and MI

The NF-κB signaling in airway epithelium is integral to mouse lung tumorigenesis induced by urethane (27), the parent compound of VC. Therefore, we sought to determine if the lung tumor inhibitory activity of I3C and MI was related to their effect on NF-κB and related proteins. For this, tissue lysates were prepared from normal lungs (vehicle-treated group) and lung tumors (VC plus I3C, VC plus MI and VC-only-treated mice) as described in the Materials and Methods section and protein levels of IkappaBα, NF-κB and Cox-2 determined by western immunobloting. As shown in Figure 4A, both doses of I3C diminished the degradation of IkappaBα and diminished the level of activated NF-κB, probably by inducing the restoration of IkappaBα. MI did not affect the expression of either IkappaBα or NF-κB. We also examined the effects of I3C and MI on the expression of Cox-2, one of the downstream targets of NF-κB. The higher dose of I3C markedly decreased VC-induced overexpression of Cox-2, whereas the lower dose of I3C and MI caused a moderate reduction.

Inhibition of VC-induced Akt activation and FAS expression by I3C and MI

Akt plays a central role in tumorigenesis by regulating the expression of metabolic, antiapoptotic, growth stimulatory and invasion-related pathways. To investigate if I3C and MI inhibit activation of Akt, levels of phospho-Akt were analyzed in normal lungs (vehicle-treated mice)

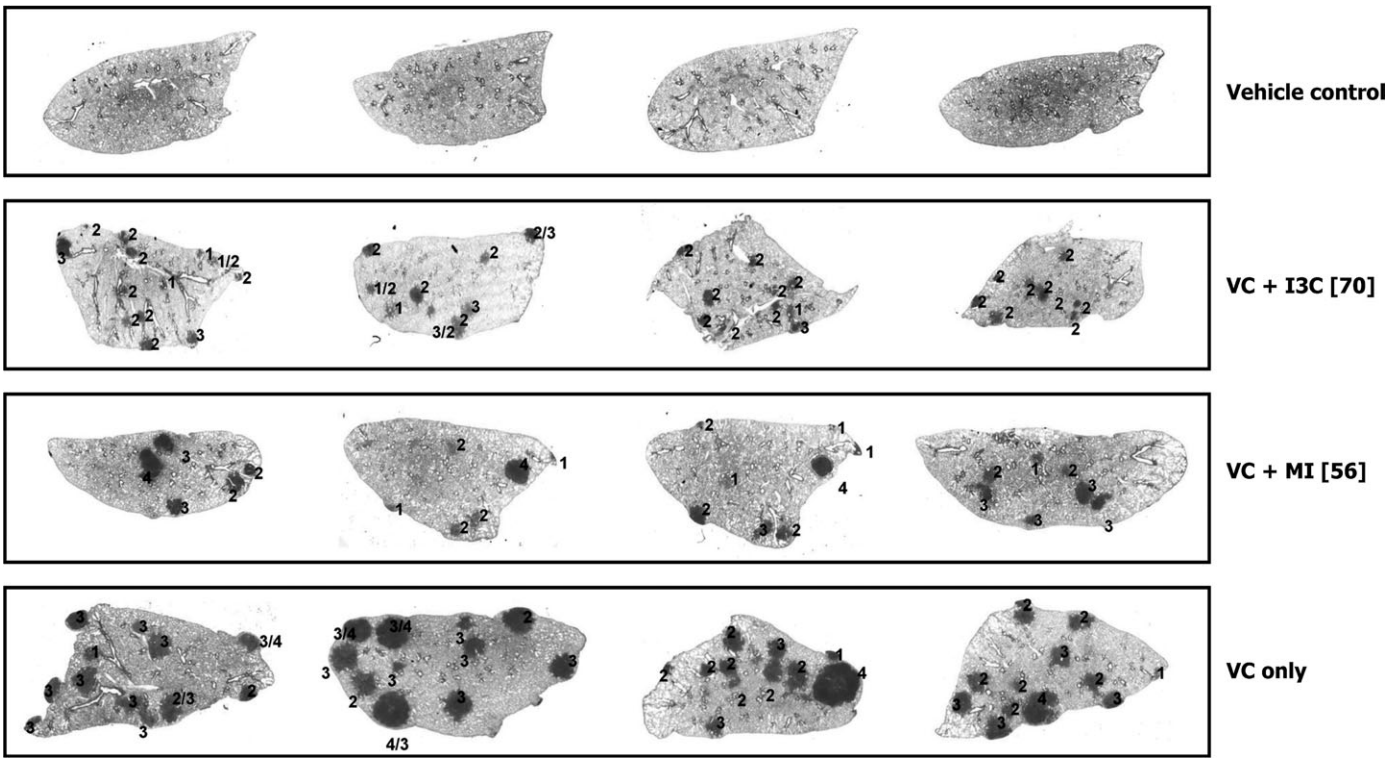

Fig. 3. Images of representative cross-sections of lung tissues from control mice and mice treated with VC plus I3C (70 μmol/g diet), VC plus MI (56 μmol/g diet) or VC alone. The numbers 1, 2, 3 and 4 represent pulmonary hyperplastic foci, adenoma, adenoma with cellular pleomorphism and adenocarcinoma, respectively.

Table II. Effects of I3C and MI on VC-induced microscopic pulmonary lesions in A/J mice[a]

Group	Carcinogen	Chemopreventive agent (dose, μmol/g diet)	No. of mice	Hyperplastic foci per mouse	Adenoma per mouse	Adenoma with cellular pleomorphism per mouse	Adenocarcinoma per mouse
1	VC	—	21	1.7 ± 1.6	4.6 ± 2.1	3.5 ± 1.6	0.6 ± 0.8
2	VC	I3C (70)	20	2.0 ± 1.7	3.6 ± 1.8	1.9 ± 1.5**	0.2 ± 0.5*
3	VC	I3C (30)	20	1.9 ± 1.5	4.6 ± 2.3	2.5 ± 1.8**	0.5 ± 0.6
4	VC	MI (56)	20	2.3 ± 1.5	2.2 ± 1.6**	2.1 ± 1.2**	0.6 ± 0.7
5	None	None	10	None	None	None	None

*$P = 0.04$; **$P < 0.0001$, compared with group 2.

[a]For the assessment of pulmonary tumor multiplicity and types of proliferative lesions, three step sections having 4 μm thickness were cut and stained with hematoxylin and eosin. Proliferative lesions were counted in each step section and the total number of each type of lesion per mouse was expressed as an average number of each lesion per section (sum of each lesion in three step sections divided by three). Proliferative lesions in the lungs were classified as hyperplastic foci, adenoma or adenocarcinoma based on recommendations published by the Mouse Models of Human Cancers Consortium [Nikitin *et al.*, (24)].

and lung tumors (VC plus I3C, VC plus MI and VC-only-treated mice). Compared with the level in mice treated with VC alone, the expression of phospho-Akt was markedly reduced in mice treated with VC plus the higher dose of I3C or MI. The lower dose of I3C did not modulate Akt activation.

Since Akt activation regulates the expression of FAS, a multifunctional metabolic enzyme that catalyzes the terminal stages in the synthesis of long-chain fatty acids, we also examined the level of this enzyme in the same lung tissues as for the phospho-Akt assay. As shown in Figure 4B, the trend in the expression of FAS paralleled that of phospho-Akt levels, suggesting a correlation between Akt activation and FAS expression in lung tumors.

Effect of I3C and MI on apoptosis-related proteins

The expression of proteins related to apoptosis was analyzed to determine if apoptotic events are induced by I3C and MI in mouse lung tumor cells. As shown in Figure 4C, in mice treated with VC plus the higher dose of I3C, a band corresponding to cleaved caspase-3 (20 kDa) was evident, indicating caspase-3 activation concomitant with an increase in cleavage of the 116 kDa PARP to an 89 kDa fragment. The effects of the lower dose of I3C or MI on caspase-3 or PARP cleavage were minimal.

Discussion

Although cessation of cigarette smoking is the best approach to reduce lung cancer mortality, the risk of lung cancer in ex-smokers remains elevated for many years after quitting (28). Therefore, approaches to reduce lung cancer in this high-risk population are urgently required. Several previous preclinical studies have investigated the ability of I3C and MI to inhibit experimentally induced lung tumorigenesis (14–17,21–23,29–31). However, almost all of these studies were terminated at the adenoma stage and it was not clear if the compound inhibits the development of pulmonary adenocarcinoma. Moreover, with the exception of one report (22), none of the studies assessed the effect of I3C when given during the

Table III. Effects of I3C and MI on the size of VC-induced pulmonary adenocarcinoma in A/J mice[a]

Group	No. of mice per group	Total number of adenocarcinoma		
		<0.1 cm^2	0.1–1.0 cm^2	>1 cm^2
Carcinogen control	21	0	22 (63%)	13 (37%)
VC + I3C (70 μmol/g diet)	20	5 (36%)*	9 (64%)	0*
VC + I3C (30 μmol/g diet)	20	0	22 (85%)*	4 (15%)*
VC + MI (56 μmol/g diet)	20	0	32 (89%)*	4 (11%)*

*$P < 0.05$ (Fisher's exact test).

[a]To determine the size of pulmonary adenocarcinoma, digital images of the lesions were taken with a Spot Insight 4 digital camera attached to a Nikon Eclipse light microscope and saved as tiff files. Subsequently, the tumor size was determined with the Image Pro program precalibrated to convert pixels into square microns according to magnification used for acquiring the image. In Image Pro, the tumor was outlined with a free hand drawing tool and the area was converted into a single object and the size of this object measured in square centimeter.

post-carcinogen treatment phase. In the present study, the chemopreventive agents were administered beginning one week after the second injection of VC and continued until week 18 of the experiment, the time period at which some of the adenoma progress into adenocarcinoma. We demonstrated that I3C reduces the multiplicity and size of pulmonary surface tumors and the incidence, multiplicity and size of pulmonary adenocarcinoma, whereas MI decreases the multiplicity and size of surface tumors and the size of adenocarcinoma. We also showed that dietary administration of I3C reduced the levels of phospho-NF-κB, Cox-2, phospho-Akt and FAS but increased proteolytic cleavage of caspase-3 and PARP in lung tumor tissues; the effect of MI was limited to modulation of phospho-Akt and FAS expression.

Classification of pulmonary surface tumors into different size categories showed that the lower multiplicity of tumors in mice given carcinogen plus I3C (70 μmol/g diet) was due to substantial reduction in the number of larger tumors. Histopathological analysis of the tumors also revealed that I3C decreased multiplicities of adenoma with cellular pleomorphism and adenocarcinoma but not hyperplastic foci or adenoma. Furthermore, adenocarcinoma lesions measuring >1 cm^2 were completely abolished. Collectively, the macroscopic and microscopic findings suggest that I3C selectively affects more advanced tumors, probably due to the higher rate of cell proliferation in these lesions. In an earlier study, Lu *et al.* (32) showed that the rate of cell proliferation is higher in mouse pulmonary adenocarcinoma than in adenoma and chemopreventive agents reduced the cell proliferation index in adenocarcinoma but not in adenoma. The selective effect of I3C on bigger tumors is potentially very important since tumor size is a key determinant of the survival of lung cancer patients (33,34). MI was less effective than the higher dose of I3C in reducing the multiplicity of larger pulmonary surface tumors and did not reduce multiplicities of adenocarcinoma but significantly reduced multiplicities of adenoma and adenoma with cellular pleomorphism and decreased the size of adenocarcinoma. These results indicate that once the tumors develop into more advanced forms, MI does not cause them to regress but inhibits only their further growth. Earlier studies on the effect of MI on pulmonary adenocarcinoma formation showed that the chemopreventive efficacy of the compound depends on when it is administered. Estensen *et al.* (26) reported that MI failed to prevent carcinoma or adenoma with progression when added to the diet 12 weeks after treatment with benzo[*a*]pyrene. Similar results were obtained when MI was given 10 weeks after exposure to VC (35). On the other hand, in the latter study, the multiplicity of adenocarcinoma was reduced from 0.67 ± 0.29 to 0.10 ± 0.10 when MI was given in the diet beginning one week before the carcinogen. In general, our results as well as those of others indicate that MI is more effective toward less-advanced lung lesions and for maximal effects, administration should begin during carcinogen exposure or immediately thereafter.

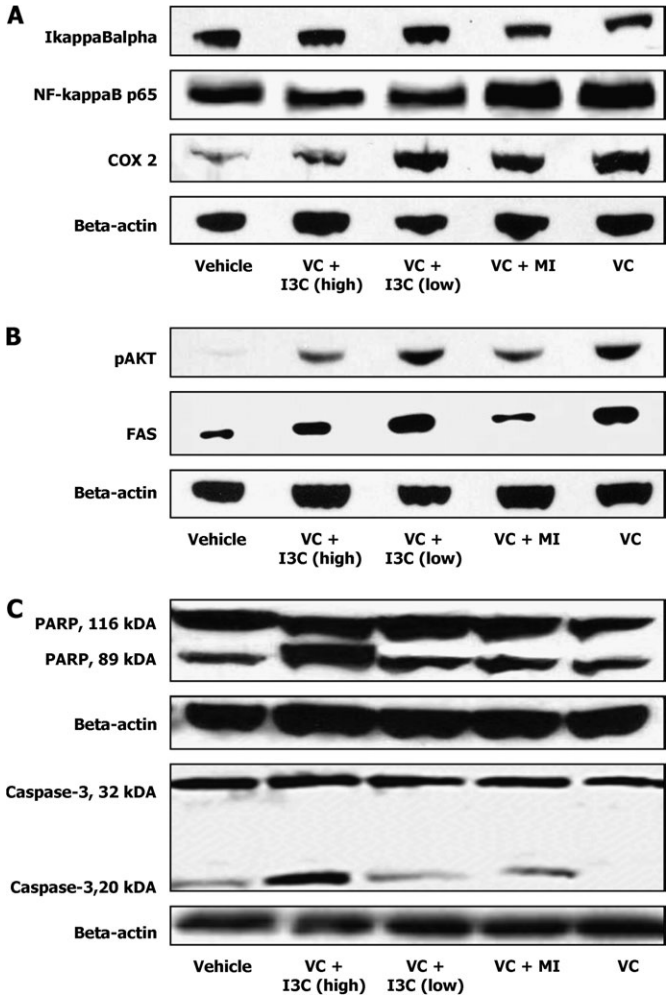

Fig. 4. Western immunoblot analyses of NF-κB-related proteins (**A**), phospho-Akt and FAS (**B**) and caspase-3 and poly ADP ribose polymerase (PARP) (**C**) in lung tissues of A/J mice. Aliquots of normal lung tissues (30 mg per mouse) or microdissected tumors (30 mg per mouse) from six mice were pooled and homogenized in ice-cold lysis buffer and processed as described in Materials and Methods and equal amounts of protein were loaded onto a 4–12% sodium dodecyl sulfate–polyacrylamide gel electrophoresis followed by immunoblot analysis and chemiluminescence detection. Equal loading of protein was confirmed by stripping the immunoblot and reprobing it for β-actin. Lanes 1, 2, 3, 4 and 5 represent lung tissue samples from vehicle-, VC plus I3C (70 μmol/g diet)-, VC plus I3C (30 μmol/g diet)-, VC plus MI (56 μmol/g diet)- and VC-only-treated mice, respectively.

The mechanisms through which I3C suppresses tumorigenesis have been extensively investigated in cell culture models and include inhibition of cell proliferation and induction of apoptosis via modulation of the Akt-NF-κB-signaling pathway, caspase activation, cyclin-dependent kinase activities, estrogen receptor signaling and endoplasmic reticulum stress (3). On the other hand, the mode of chemopreventive activity of MI is largely unknown. To better understand the molecular effects of I3C and MI in mouse lung tumors, we examined the effects of I3C and MI on key proteins involved in NF-κB, Akt and apoptosis pathways. NF-κB is present in the cytoplasm in an inactive form as a heterotrimer consisting of p50, p65 and IkappaBα subunits. Proteolytic degradation of IkappaBα by IkappaB kinase leads to activation and nuclear translocation of NF-κB. Activation of the NF-κB pathway leads to upregulation of several genes involved in tumor initiation, promotion and progression (36), including Cox-2, which has an NF-κB-binding site on its promoter and is implicated in angiogenesis, tumor invasion, resistance to apoptosis

and suppression of antitumor immunity (37). In the present study, we showed that I3C is an effective inhibitor of NF-κB activation and suppressor of Cox-2 expression, indicating the promise of this agent as a chemopreventive agent against lung cancer. Indeed, earlier studies in *in vitro* models demonstrated suppression of constitutive and induced NF-κB activation and NF-κB-regulated genes by I3C in breast, prostate and blood cancer cells (38–40).

Phospho-Akt is another potentially important target for the chemoprevention of lung cancer since it is frequently overexpressed in non-small cell carcinoma and preneoplastic bronchial lesions (41). Phospho-Akt plays a prominent role in several processes thought to be critical in lung tumorigenesis, including increased cell proliferation, inhibition of programmed cell death, telomerase activation and promotion of angiogenesis and tumor cell invasiveness (42). Activation of Akt is molecularly linked to overexpression of FAS (43), a key metabolic enzyme that catalyzes the synthesis of long-chain fatty acids and is highly expressed in preneoplastic and neoplastic lung lesions (44,45). Recently, FAS has been shown to be an oncogene and its oncogenic effect is mediated through inhibition of the intrinsic pathway of apoptosis (46). The suppression of phospho-Akt and FAS levels by both I3C and MI in the present study could explain, at least partly, the reduction in the size of tumors. In our earlier study, we observed that I3C and MI downregulate phospho-Akt and FAS in lung tissues of A/J mice treated with 4-(methylnitrosamino)-1-(3-pyridyl)-1-butanone plus benzo[*a*]pyrene (21–23). The present findings together with our previous reports indicate that phospho-Akt and FAS are important targets for the chemopreventive effect of I3C and MI. However, the molecular mechanisms behind this effect need further investigation. Also, the potential synergy of I3C and MI in inhibiting phospho-Akt and FAS expression is an interesting research area.

A hallmark of the apoptotic process is the cleavage of PARP, an enzyme implicated in DNA damage and repair mechanisms. In the present study, the higher dose of I3C markedly activated caspase-3, the executioner caspase that catalyzes the specific cleavage of PARP, and PARP, suggesting that apoptosis is the link between the chemopreventive role of I3C and the reduction in the multiplicity of carcinoma in VC plus I3C-treated mice. Moreover, blocking of Akt and NF-κB activation has been shown to play a role in I3C-induced apoptosis (4,47).

In summary, we showed here that both I3C and MI inhibit the development of VC-induced pulmonary adenocarcinoma in A/J mice, but the effects of I3C were markedly stronger than that of MI. The higher efficacy of I3C against pulmonary adenocarcinoma is in line with the many available reports in which I3C or its metabolite DIM showed preventive/therapeutic effects against late stages of carcinogenesis (inhibition of tumor invasion and angiogenesis and inhibition of proliferation and induction of apoptosis in cancer cells). On the other hand, MI failed to alter viability or proliferation of cancer cells (19) but showed remarkable preventive effects during the early stage of lung carcinogenesis (14–18). These results imply that, for the design of human lung cancer prevention clinical trials, I3C could be used for the chemoprevention of early and advanced pulmonary lesions, but the use of MI should be limited to chemoprevention of early pulmonary lesions. An interesting question would be the potential synergy in the chemopreventive effect of I3C and MI. Currently, we are trying to address this issue.

Funding

National Cancer Institute (CA-102502 to S.S.H.).

Acknowledgements

We thank Michael Jarcho for his help in the western analysis.

Conflict of Interest Statement: None declared.

References

1. Parkin,D.M. *et al*. (2005) Global cancer statistics, 2002. *CA Cancer J. Clin.*, **55**, 74–108.
2. Jemal,A. *et al*. (2008) Cancer Statistics, 2008. *CA Cancer J. Clin.*, **58**, 71–96.
3. International Agency for Research on Cancer. (2004) *Cruciferous Vegetables, Isothiocyanates and Indoles. IARC Handbooks of Cancer Prevention*. IARC Printing Press, Lyon, Vol. 9, pp. 171–176.
4. Rahman,R.M. *et al*. (2006) Therapeutic intervention of experimental breast bone metastasis by indole-3-carbinol in SCID-human mouse model. *Mol. Cancer Ther.*, **5**, 2747–2756.
5. Bjeldanes,L.F. *et al*. (1991) Aromatic hydrocarbon receptor agonist generated from indole-3-carbinol *in vitro* and *in vivo*: comparisons with 2,3,7,8-tetrachlorodibenzo-p-dioxin. *Proc. Natl Acad. Sci. USA*, **88**, 9543–9547.
6. Li,Y. *et al*. (2005) Selective growth of regulatory and pro-apoptotic effects of 3,3′-diindolylmethane is mediated by Akt and NF-kappaB pathways in prostate cancer cells. *Front. Biosci.*, **10**, 236–243.
7. Nachshon-Kedmi,M. *et al*. (2004) Therapeutic activity of 3,3′-diindolylmethane on prostate cancer in an *in vivo* model. *Prostate*, **61**, 153–160.
8. Abdelrahim,M. *et al*. (2005) 3,3′-Diindolylmethane and its derivatives induce apoptosis in pancreatic cancer cells through endoplasmic reticulum stress-dependent up-regulation of DR5. *Carcinogenesis*, **27**, 717–728.
9. Rahman,K.W. *et al*. (2006) Gene expression profiling revealed survivin as a target of 3,3′-diindolylmethane-induced cell growth inhibition and apoptosis in breast cancer cells. *Cancer Res.*, **66**, 4952–4960.
10. Rahman,K.M. *et al*. (2007) Inactivation of NF-kappaB by 3,3′-diindolylmethane contributes to increased apoptosis induced by chemotherapeutic agent in breast cancer cells. *Mol. Cancer Ther.*, **6**, 2757–2765.
11. Kong,D. *et al*. (2007) Inhibition of angiogenesis and invasion by 3,3′-diindolylmethane is mediated by NF-kappaB downstream target genes MMP-9 and uPA that regulated bioavailability of vascular endothelial growth factor in prostate cancer. *Cancer Res.*, **67**, 3310–3319.
12. Chang,X. *et al*. (2006) Inhibition of growth factor-induced Ras signaling in vascular endothelial cells and angiogenesis by 3,3′-diindolylmethane. *Carcinogenesis*, **27**, 541–550.
13. Banerjee,S. *et al*. (2009) 3,3′-Diindolylmethane enhances chemosensitivity of multiple chemotherapeutic agents in pancreatic cancer. *Cancer Res.*, **69**, 5592–5600.
14. Estensen,R.D. *et al*. (1993) Studies of chemopreventive effects of *myo*-inositol on benzo[*a*]pyrene-induced neoplasia of the lung and forestomach of female A/J mice. *Carcinogenesis*, **14**, 1975–1977.
15. Wattenberg,L.W. *et al*. (1996) Chemopreventive effects of *myo*-mositol and dexamethasone on benzo[a]pyrene and 4-(methylnitrosamino)-1-(3-pyridyl)-1-butanone-induced pulmonary carcinogenesis in female A/J mice. *Cancer Res.*, **56**, 5132–5135.
16. Hecht,S.S. *et al*. (2001) Dose-response study of *myo*-inositol as an inhibitor of lung tumorigenesis induced in A/J mice by benzo(*a*)pyrene and 4-(methylnitrosamino)-1-(3-pyridyl)-1-butanone. *Cancer Lett.*, **167**, 1–6.
17. Hecht,S.S. *et al*. (2002) Inhibition of lung tumorigenesis in A/J mice by *N*-acetyl-*S*-(*N*-2-phenethylcarbamoyl)-L-cysteine and *myo*-inositol, individually and in combination. *Carcinogenesis*, **23**, 1255–1261.
18. Lam,S. *et al*. (2006) A phase I study of *myo*-inositol for lung cancer chemoprevention. *Cancer Epidemiol. Biomarkers Prev.*, **15**, 1526–1531.
19. Jyonouchi,H. *et al*. (1999) Effects of anti-7,8-dihydroxy-9,10-epoxy-7,8,9,10-tetrahydrobenzo[a]pyrene on human small airway epithelial cells and the protective effects of *myo*-inositol. *Carcinogenesis*, **20**, 139–145.
20. Han,W. *et al*. (2009) The chemopreventive agent myoinositol inhibits Akt and extracellular signal-regulated kinase in bronchial lesions from heavy smokers. *Cancer Prev. Res.*, **2**, 370–376.
21. Kassie,F. *et al*. (2007) Indole-3-carbinol inhibits 4-(methylnitrosamino)-1-(3-pyridyl)-1-butanone plus benzo(*a*)pyrene-induced lung tumorigenesis in A/J mice and modulates carcinogen-induced alterations in protein levels. *Cancer Res.*, **67**, 6502–6511.
22. Kassie,F. *et al*. (2008) Dose-dependent inhibition of tobacco smoke carcinogen-induced lung tumorigenesis in A/J mice by indole-3-carbinol. *Cancer Prev. Res.*, **1**, 568–576.
23. Kassie,F. *et al*. (2008) Combinations of *N*-Acetyl-*S*-(*N*-2-phenethylthiocarbamoyl)-L-cysteine and *myo*-inositol inhibit tobacco smoke carcinogen-induced lung adenocarcinoma in A/J mice. *Cancer Prev. Res.*, **1**, 285–297.
24. Nikitin,A.Y. *et al*. (2004) Classification of proliferative pulmonary lesions of the mouse: recommendations of the mouse models of human cancers consortium. *Cancer Res.*, **64**, 2307–2316.
25. Conaway,C.C. *et al*. (2005) Phenethyl isothiocyanate and sulforaphane and their *N*-acetylcysteine conjugates inhibit malignant progression of lung adenomas induced by tobacco carcinogens in A/J mice. *Cancer Res.*, **65**, 8548–8557.
26. Estensen,R.D. *et al*. (2004) Effect of chemopreventive agents on separate stages of progression of benzo[*a*]pyrene induced lung tumors in A/J mice. *Carcinogenesis*, **25**, 197–201.

27. Stathopoulos,G.T. *et al*. (2007) Epithelial NF-kappaB activation promotes urethane-induced lung tumorigenesis. *Proc. Natl Acad. Sci. USA*, **104**, 18514–18519.
28. Blot,W.J. *et al*. (1996) Cancers of the lung and pleura. In Schottenfeld,D. and Fraumeni,J.F. (eds.) *Cancer Epidemiology and Prevention*. Oxford University Press, New York, NY, pp. 637–665.
29. Morse,M.A. *et al*. (1990) Effects of indole-3-carbinol on lung tumorigenesis and DNA methylation induced by 4-(methylnitrosamino)-1-(3-pyridyl)-1-butanone (NNK) and on the metabolism and disposition of NNK in A/J mice. *Cancer Res.*, **50**, 2613–2617.
30. El Bayoumy,K. *et al*. (1996) Effects of 1,4-phenylenebis (methylene)selenocyanate, phenethyl isothiocyanate, indole-3-carbinol, and D-limonene individually and in combination on the tumorigenicity of the tobacco-specific nitrosamine 4-(methylnitrosamino)-1-(3-pyridyl)-1-butanone in A/J mouse lung. *Anticancer Res.*, **16**, 2709–2712.
31. Yu,Z. *et al*. (2006) Indole-3-carbinol in the maternal diet provides chemoprotection for the fetus against transplacental carcinogenesis by the polycyclic aromatic hydrocarbon dibenzo[a,l]pyrene. *Carcinogenesis*, **27**, 2116–2123.
32. Lu,G. *et al*. (2006) Inhibition of adenoma progression to adenocarcinoma in a 4-(methylnitrosamino)-1-(3-pyridyl)-1-butanone–induced lung tumorigenesis model in A/J mice by tea polyphenols and caffeine. *Cancer Res.*, **66**, 11494–11501.
33. Port,J.L. *et al*. (2003) Tumor size predicts survival within stage IA non-small cell lung cancer. *Chest*, **124**, 1828–1833.
34. Birim,O. *et al*. (2005) Survival after pathological stage IA nonsmall cell lung cancer: tumor size matters. *Ann. Thorac. Surg.*, **79**, 1137–1141.
35. Gunning,W.T. *et al*. (2000) Chemoprevention of vinyl carbamate-induced lung tumors in strain A mice. *Exp. Lung Res.*, **26**, 757–772.
36. Pahl,H.L. (1999) Activators and target genes of Rel/NF-kappaB transcription factors. *Oncogene*, **18**, 6853–6866.
37. Sandler,A.B. *et al*. (2004) COX-2 inhibition and lung cancer. *Semin. Oncol.*, **31**, 45–52.
38. Chinni,S.R. *et al*. (2001) Indole-3-carbinol (I3C) induced cell growth inhibition, G1 cell cycle arrest and apoptosis in prostate cancer cells. *Oncogene*, **20**, 2927–2936.
39. Takada,Y. *et al*. (2005) Indole-3-carbinol suppresses NF-κB and IκBα kinase activation, causing inhibition of expression of NF-κB-regulated antiapoptotic and metastatic gene products and enhancement of apoptosis in myeloid and leukemia cells. *Blood*, **106**, 641–649.
40. Rahman,K.M.W. *et al*. (2000) Translocation of Bax to mitochondria induces apoptotic cell death in indole-3-carbinol (I3C) treated breast cancer cells. *Oncogene*, **19**, 5764–5771.
41. Balsara,B.R. *et al*. (2004) Frequent activation of Akt in non-small cell lung carcinomas and preneoplastic bronchial lesions. *Carcinogenesis*, **25**, 2053–2059.
42. Testa,J.R. *et al*. (2001) AKT plays a central role in tumorigenesis. *Proc. Natl Acad. Sci. USA*, **98**, 10983–10985.
43. Sande,T.V. *et al*. (2002) Role of the phosphatidylinositol 3′-kinase/PTEN/Akt kinase pathway in the overexpression of fatty acid synthase in LNCaP prostate cancer cells. *Cancer Res.*, **62**, 642–646.
44. Orita,H. *et al*. (2007) Selective inhibition of fatty acid synthase for lung cancer treatment. *Clin. Cancer Res.*, **13**, 7139–7145.
45. Orita,H. *et al*. (2008) Inhibiting fatty acid synthase for chemoprevention of chemically induced lung tumors. *Clin. Cancer Res.*, **14**, 2458–2464.
46. Migita,T. *et al*. (2009) Fatty acid synthase: a metabolic enzyme and candidate oncogene in prostate cancer. *J. Natl Cancer Inst.*, **101**, 519–532.
47. Rahman,K.W. *et al*. (2004) Inactivation of Akt and NF-kB plays important roles during I3C-induced apoptosis in breast cancer cells. *Nutr. Cancer*, **48**, 84–94.

Received May 18, 2009; revised June 24, 2009; accepted June 25, 2009